Nuclear Physics **A480** (1988) 285–311
North-Holland, Amsterdam

THE ^{52,54}Cr(p, n)^{52,54}Mn AND ^{57,58}Fe(p, n)^{57,58}Co REACTIONS AT $E_p = 120$ MeV

D. WANG and J. RAPAPORT

Ohio University, Athens, OH 45701, *USA*

D.J. HOREN

Oak Ridge National Laboratory, Oak Ridge, TN 37830, *USA*

B.A. BROWN

Michigan State University, East Lansing, MI 48824, *USA*

C. GAARDE

Niels Bohr Institute, Copenhagen, Denmark

C.D. GOODMAN

Indiana University, Bloomington, KN 47405, *USA*

E. SUGARBAKER

Ohio State University, Columbus, OH 43215, *USA*

T.N. TADDEUCCI

Los Alamos National Laboratory, Los Alamos, NM 87545, *USA*

Received 9 November 1987

Abstract: Differential cross sections for the (p, n) reaction on ^{52,54}Cr and ^{57,58}Fe have been measured for angles up to $\theta_{lab} = 10.5°$ and 14.6°, respectively, using 120 MeV protons. The observed angular distributions are used to evaluate the location and strength of Gamow-Teller resonances. A shell-model calculation of this strength distribution is presented and compared with the experimental results. The M1 strength for ^{52}Cr is also calculated and compared with available results from (e, e′) and (p, p′) experiments. A comparison is made with other lf $_{7/2}$nuclei.

NUCLEAR REACTIONS ^{52,54}Cr, ^{57,58}Fe(p, n), $E = 120$ MeV; measured $\sigma(\theta)$. ^{52,54}Mn, ^{57,58}Co deduced Gamow-Teller resonances, transition strengths. Enriched targets. DWIA analysis.

1. Introduction

The observation of spin modes of excitation in nuclei, in particular those with low-multipolarity, has received large interest in recent years. Empirically determined proportionality factors have been used to relate intermediate energy zero-degree (p, n) cross sections to the Fermi (F) and Gamow-Teller (GT) strengths for the corresponding transitions [1]). Studies of nuclei throughout the periodic table have

0375-9474/88/$03.50

established that the total observed Gamow-Teller strength, S_{β^-}, is only a fraction of the strength required by the GT sum rule limit [2,3]). This quenching of the spin-isospin strength which has been observed most clearly in the (p, n) reaction has also been studied by exciting the magnetic dipole mode by means of high resolution inelastic proton scattering, inelastic electron scattering and resonance fluorescence measurements. Several mechanisms have been suggested to explain the depletion of strength in the region where it is predicted by the shell model. One school of authors suggests that the strength in the sharp states becomes distributed by mixing with multiparticle-multihole configurations into a continuum that cannot readily be distinguished from "background". These multiparticle-multihole configurations are not included in standard shell-model calculations. Another school of authors suggests that coupling to delta-hole configurations, also not included in shell-model calculations, redistributes the strength to very high excitations [see ref. [4]) and references therein].

For nuclei in the $1f_{7/2}$ shell region the valence neutrons and protons are filling the same subshell. Therefore, model calculations predict significant unblocked S_{β^+} strength, which, by the sum rule [2]) $S_{\beta^-} - S_{\beta^+} = 3(N-Z)$, implies a total strength, S_{β^-}, greater than $3(N-Z)$. Zero-degree (p, n) spectra can be compared to model calculations of GT strength [5]). In addition the models also provide predictions of the distribution of M1 strength which can be compared to data from large angle inelastic electron scattering and small angle inelastic proton scattering. Recent (n, p) results obtained at intermediate energies of $1f_{7/2}$ nuclei [6]) also provide an empirical evaluation of the S_{β^+} strength.

The nuclei ^{48}Ca, ^{50}Ti, ^{52}Cr and ^{54}Fe are all $N = 28$ isotones for which the observation of M1 resonances excited either via electron scattering [7]) or with medium energy protons [8]) has been reported. A very complete study of M1 excitations in ^{50}Ti, ^{52}Cr and ^{54}Fe has been reported by Sober *et al.* [9]). Additionally, lower energy inelastic proton scattering to 1^+ states in these nuclei has been reported by Fujiwara *et al.* [10]).

The location and strength of (p, n) GT resonances in $1f_{7/2}$ nuclei have been presented in several references; in ^{48}Ca by Anderson *et al.* [11]); in ^{51}V by Rapaport *et al.* [5]) and in ^{54,56}Fe and ^{58,60}Ni by Rapaport *et al.* [12]).

In the case of ^{52}Cr, Eulenberg *et al.* [7]) report a value $\sum B(\mathrm{M1})\uparrow = 5.1 \pm 0.5\ \mu_n^2$ for the summed M1 strength while the recent inelastic electron scattering experiment by Sober *et al.* [9]) indicates a higher "recommended value" $\sum B(\mathrm{M1})\uparrow = 8.1 \pm 0.8\ \mu_n^2$. In the same paper, Sober *et al.* [9]) report on 1-particle-1-hole shell-model calculations. Assuming free-nucleon g-factors a value $\sum B(\mathrm{M1})\uparrow = 19.1 \mu_n^2$ is calculated if all final states are included.

In the high resolution (p, p′) measurements [8]), the summed (p, p′) cross section for the assigned M1 states observed at $\theta_{lab} = 4°$ and $E_p = 201$ MeV is $\sum \sigma(\mathrm{p, p'}) = 5.3 \pm 0.7$ mb/sr. A corresponding shell-model calculation by B.A. Brown is reported in ref. [5]). The single 1-particle-1-hole shell-model wave functions yield a distorted-wave

impulse approximation (DWIA) cross section sum of $\sum\sigma(p, p') = 19.0$ mb/sr. By using Towner and Khanna effective operators [13]), which include non-nucleonic degrees of freedom and shell-model configuration effects, the calculated DWIA value is reduced to 14.7 mb/sr, $\sum\sigma(p, p')$ still a factor of three larger than that reported from (p, p') studies. The mechanisms suggested to explain the quenching of GT strength would also quench M1 strength and it seems likely that the observed M1 quenching is due to a common mechanism operating for M1 and GT transitions.

In the present work we present 120 MeV (p, n) data on ^{52,54}Cr and on ^{57,58}Fe. The measured angular distributions are used to select $\Delta L = 0$ transitions for which the experimentally observed GT strength is estimated and then compared with shell-model calculations.

2. Experimental procedure

The experiment was performed using the beam swinger neutron time-of-flight facility at the Indiana University Cyclotron Facility [14]). Large volume time-compensated plastic scintillators [15]) were located along the zero-degree beam line with respect to an undeflected proton beam at a distance of approximately 130 m. Additional details about the experimental set-up may be found in ref. [14]). Sub-nanosecond time resolution was achieved, which is equivalent to an overall energy resolution of about 300 keV. The outgoing neutrons were observed at $\theta_{lab} = 0°$, 4.0°, 8.2°, 10.5° and 14.6°. The electronics and data acquisition were similar to that described in ref. [16]).

The thickness and enrichments of the metallic foils used as self-supported targets are given in table 1. Targets of ^{7}Li and ^{12}C were used under identical experimental conditions to observe neutrons and obtain an energy calibration as well as the absolute efficiency of the neutron detectors. The method described in ref. [17]) was employed to obtain an absolute efficiency for the neutron detectors. A recent value [18]) for the ^{7}Li(p, n)^{7}Be (g.s. + 0.43 MeV) total cross section was used to obtain the zero-degree differential cross section ($\sigma_{c.m.}(0°) = 28 \pm 2$ mb/sr) [1]) needed for this normalization procedure.

TABLE 1

Composition of metallic foils used as targets

Isotopes	Total thickness	Enrichment	
^{52}Cr	25.4 ± 1.8	99%	
^{54}Cr	27.0 ± 3.0	91%	(9% ^{52}Cr)
^{57}Fe	37 ± 1.0	90%	
^{58}Fe	40.0 ± 1.0	92%	(8% ^{57}Fe)

3. Data and experimental results

Zero-degree spectra of c.m. cross section versus outgoing neutron energy are shown in figs. 1 and 2. The values shown for absolute (p, n) cross sections are obtained directly from the ^{7}Li(p, n)^{7}Be calibration with no further correction necessary for neutron energies near those from the calibration reaction. For lower energy neutrons, calculated energy-dependent corrections were applied for the detector efficiency and the neutron attenuation in the flight path between the target and the detector. These corrections were about 10% for outgoing neutrons corresponding to 20 MeV excitation energy in the final nucleus.

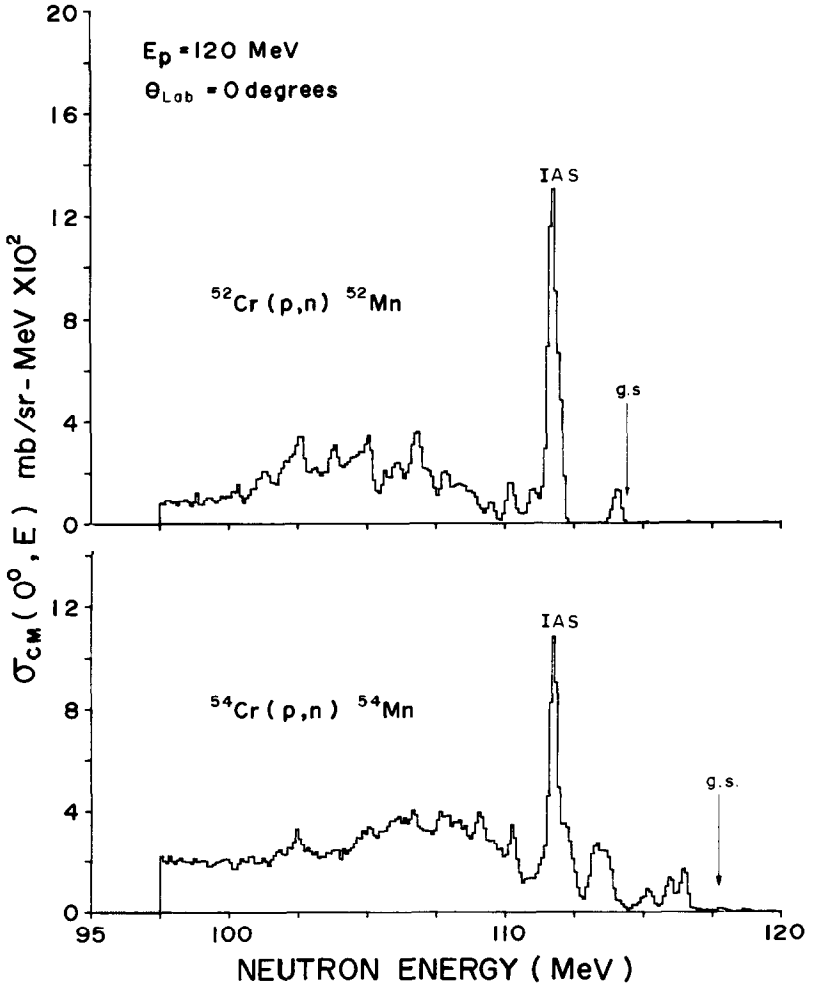

Fig. 1. Differential cross section versus outgoing neutron energy for (top) ^{52}Cr(p, n)^{52}Mn and (bottom) ^{54}Cr(p, n)^{54}Mn at $\theta = 0°$ and $E_p = 120$ MeV. The most prominent peaks in both spectra correspond to the isobaric analog state transitions.

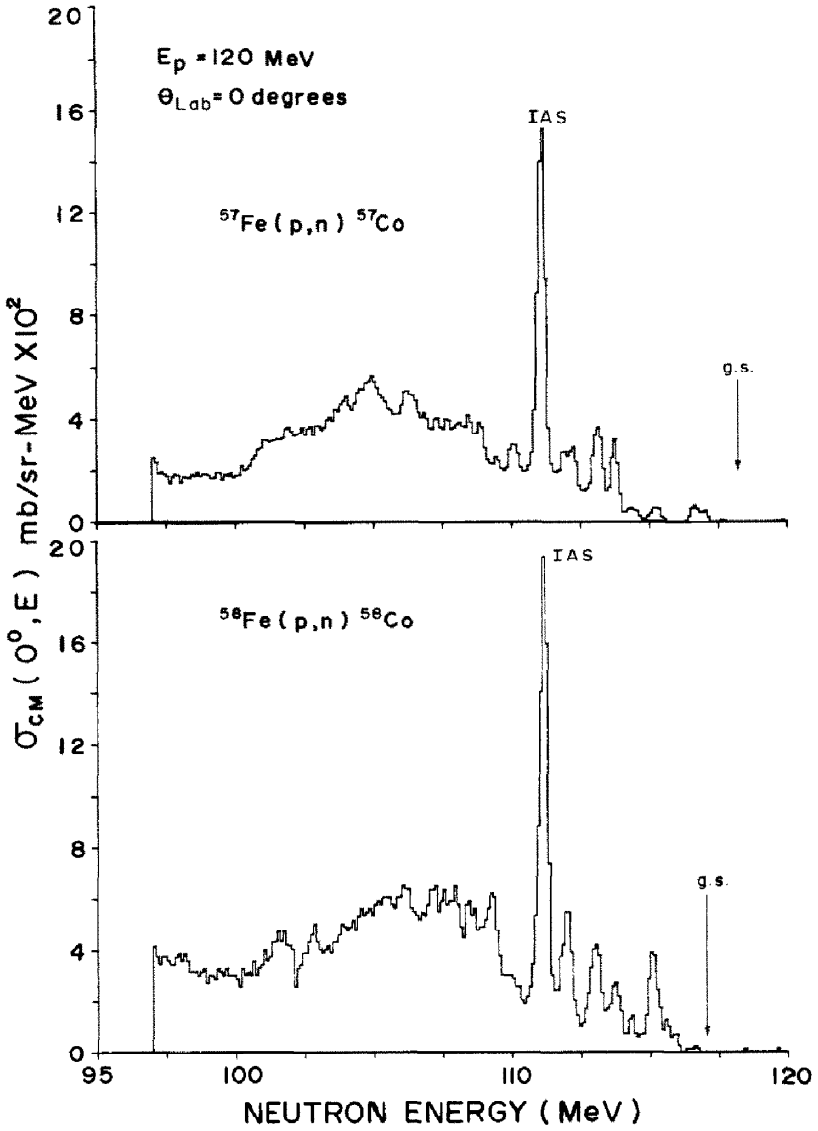

Fig. 2. Differential cross section versus outgoing neutron energy for (top) ^{57}Fe(p, n)^{57}Co and (bottom) ^{58}Fe(p, n)^{58}Co at $\theta = 0°$ and $E_p = 120$ MeV. The prominent peaks in both spectra correspond to the isobaric analog state transitions.

Whenever possible the peak areas were extracted by fitting the region of interest with a gaussian peak shape and a linear background function. The excitation energy uncertainty of the observed neutron groups is estimated to be about 100 keV.

In the next few paragraphs we will present data and results for each of the studied nuclei.

3.1. THE ^{52}Cr(p, n)^{52}Mn REACTION

A zero-degree spectrum for this reaction is presented in the top part of fig. 1. The most prominent structure in the spectrum is the excitation of the isobaric analog state (IAS) in ^{52}Mn at $E_x = 2.93$ MeV [ref. [19])]. The measured differential cross sections for transitions up to 5 MeV excitation energy are shown in fig. 3. The

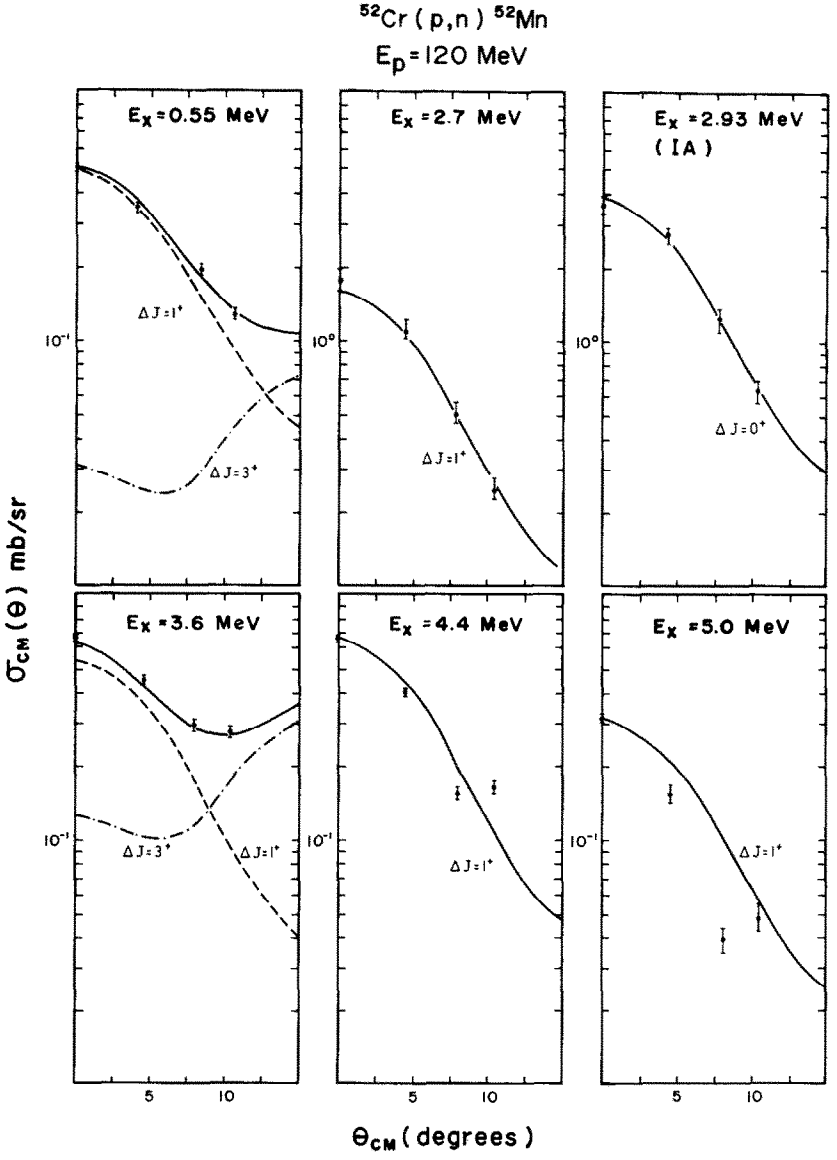

Fig. 3. Angular distributions for neutron groups observed in the ^{52}Cr(p, n)^{52}Mn reaction at E_p = 120 MeV. The lines represent DWIA calculations for the indicated ΔJ transfers.

neutron group at $E_x = 0.55$ MeV has an angular distribution characteristic of $\Delta J^\pi = 1^+$ transfer and arises mainly from the known 1^+ state in ^{52}Mn at 0.546 MeV [ref. [19])]. The indicated $\Delta J^\pi = 3^+$ admixture can arise from two $J^\pi = 3^+$ states in ^{52}Mn reported at 0.825 and 0.884 MeV [ref. [19])] that may be excited but not well resolved with the present experimental resolution. The ^{52}Mn (1^+, 0.546 MeV) state is fed in the ^{52}Fe(g.s.) beta decay with a reported [19]) $\log ft = 4.589 \pm 0.018$.

Several two particle stripping and pick-up reactions have been used to study excited states in ^{52}Mn [ref. [19])]. In particular, the ^{54}Fe(d, α)^{52}Mn reaction is of interest. The ground state (g.s.) of the ^{54}Fe nucleus has $J^\pi = 0^+$ and isospin $T_z = 1$. Because the (d, α) reaction does not transfer isospin, only $T = 1$ states in ^{52}Mn are excited in this reaction. The following states, below 4.8 MeV excitation, are reported [19]) with $J^\pi = 1^+$ in the ^{54}Fe(d, α)^{52}Mn reaction: 0.55, 2.63, 3.57 and 4.38 MeV. Neutron groups exhibiting the characteristic $\Delta J^\pi = 1^+$ angular distribution component are also observed at these energies in the present experiment. The measured differential cross sections are presented in fig. 3. The neutron group at 5.0 MeV (fig. 3) may correspond to the excitation of the 1^+, 4.953 MeV state reported in the ^{50}Cr(^{3}He, p)^{52}Mn reaction [19]).

The correspondence of neutron groups at excitation energies above 5.0 MeV with known states in ^{52}Mn is not straightforward and is not attempted. Above $E_x =$ 5.0 MeV, the measured differential cross sections for 1.0 MeV energy bins are used to estimate the $\Delta L = 0$ cross section contribution in the zero-degree spectrum using the multipole decomposition method. These values are used to estimate the GT strength in the excitation energy region between 5 and 15 MeV. A summary of location and strengths of GT transitions is shown in table 2. A more extensive analysis of the $\Delta L = 0$ spectrum is discussed in sect. 4.4.

3.2. THE ^{54}Cr(p, n)^{54}Mn REACTION

A zero-degree spectrum of differential cross section versus outgoing neutron energy for the ^{54}Cr(p, n)^{54}Mn reaction is presented at the bottom of fig. 1. The ^{54}Cr target had a 9% ^{52}Cr contamination. Since the ^{52}Cr(p, n)^{52}Mn reaction was measured under identical conditions, normalized ^{52}Cr(p, n)^{52}Mn spectra were subtracted from corresponding ^{54}Cr(p, n)^{54}Mn spectra to remove the ^{52}Cr contributions. The dominant peak in the zero-degree spectrum corresponds to the excitation of the IAS at $E_x = 6.15$ MeV in ^{54}Mn [ref. [20])]. The first neutron group observed in the zero-degree spectrum (fig. 1) corresponds to $\Delta J = 1^+$ transfer at an excitation energy of about 1.4 MeV. There are two 1^+ states in ^{54}Mn reported [20]) at excitation energies of 1.391 and 1.454 MeV, respectively.

The second neutron group in the bottom half of fig. 1 seems to correspond to an excited 1^+ state reported at 1.922 MeV. Excited 1^+ states reported at 1.634 and 1.649 MeV [ref. [20])] may also be excited but would have cross sections much smaller than the previously mentioned neutron groups. The energy resolution achieved in

TABLE 2

^{52}Cr(p, n)^{52}Mn Reaction ($E_p = 120$ MeV)
$L = 0$ transitions
Zero-degree cross sections and transition strengths

Neutron group E_x(MeV) [a]	$\sigma_{c.m.}(0°)$ [b] (mb/sr)	B(GT)	B(F)
0.55	0.51	0.094	
2.7	1.76	0.35	
2.93 [d]	3.7		4.0
3.6, 3.8	0.68	0.13	
4.4, 4.6	0.66	0.12	
5.0	0.32	0.06	
5.6, 17.0		5.1 [c]	
		$\sum B(\mathrm{GT}) = 5.9 \pm 1.5$	

[a]) Estimated location of neutron group centroid; uncertainty ±0.1 MeV.
[b]) Estimated cross section of corresponding neutron group; uncertainty ±15%
[c]) Value calculated using 1 MeV interval histogram (see fig. 7).
[d]) Isobaric analog transition.

the present experiment is not good enough to resolve all of these transitions. The measured differential cross sections for neutron groups up to 6.15 MeV excitation energy in ^{54}Mn are presented in fig. 4. For excitation energies above the IAS ($E_x = 6.15$ MeV), no attempt has been made to identify neutron groups. However, the measured angular distributions in 1 MeV energy bins have been used to estimate the $\Delta L = 0$ cross section contribution in the zero-degree spectrum; these values are used to estimate the GT strength in the excitation energy region between 6 and 18 MeV. Transitions characterized with $\Delta J = 1^+$ and their corresponding GT strengths are summarized in table 3.

3.3. THE ^{57}Fe(p, n)^{57}Co REACTION

The zero-degree spectrum for this reaction is presented at the top part of fig. 2. The excitation of the IAS at $E_x = 7.3$ MeV is the dominant feature of the spectrum. Because of the high density of states in ^{57}Co, no attempt was made to identify observed neutron groups with states in ^{57}Co. Differential cross sections for the indicated neutron groups are shown in fig. 5. The presence of a $\Delta J^\pi = 1^+$ transfer implies the excitation of states in ^{57}Co with either $J^\pi = \frac{1}{2}^-$ *or* $\frac{3}{2}^-$. Above 6 MeV excitation energy non $\Delta L = 0$ contributions to the zero-degree spectrum were obtained from the measured angular distribution. A location and strengths of GT transitions is shown in table 4.

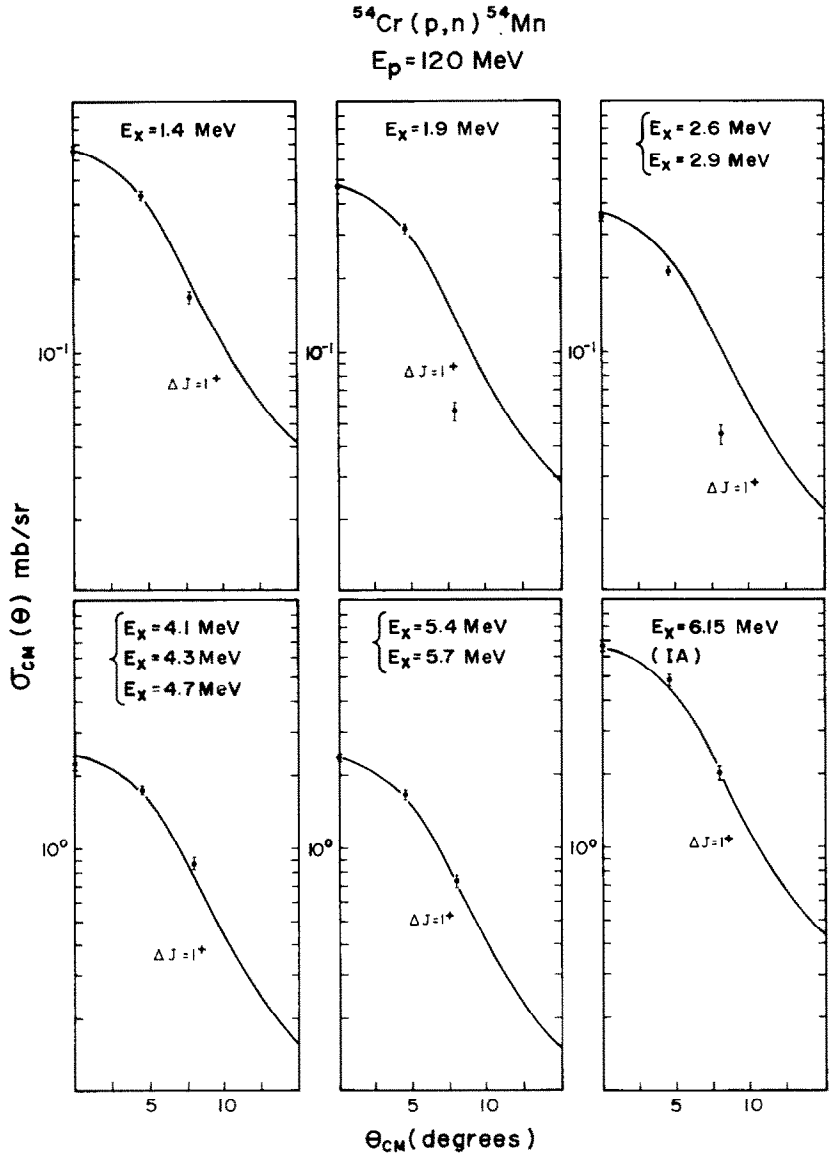

Fig. 4. Angular distributuions for neutron groups observed in the ^{54}Cr(p, n)^{54}Mn reaction at E_p = 120 MeV. The solid lines are $\Delta J = 1^+$ DWIA calculations.

3.4. THE ^{58}Fe(p, n)^{58}Co REACTION

A zero-degree spectrum for this reaction is presented in the bottom of fig. 2. Approximately 8% of ^{57}Fe was present in the ^{58}Fe target used in this experiment. Properly normalized ^{57}Fe(p, n)^{57}Co spectra were used to remove the contributions

TABLE 3

^{54}Cr(p, n)^{54}Mn Reaction ($E_p = 120$ MeV)
$L = 0$ transitions
Zero-degree cross sections and transitions strengths

Neutron group E_x (MeV) [a]	$\sigma_{c.m.}(0°)$ [b] (mb/sr)	B(GT)	B(F)
1.40	0.66	0.12	
1.90	0.47	0.084	
2.60, 2.90	0.36	0.064	
4.10, 4.30, 4.70	2.26	0.45	
5.40, 5.70	2.4	0.45	
6.15 [d]	6.8		6.0
5.7, 18.0		6.5 [c]	
		$\sum B(\mathrm{GT}) = 7.7 \pm 1.9$	

[a]) Estimated location of neutron group centroid; uncertainty ±0.1 MeV.
[b]) Estimated cross section of corresponding neutron group; uncertainty ±15%.
[c]) Value calculated using 1 MeV interval histogram (see fig. 7).
[d]) Isobaric analog transition.

due to ^{57}Fe in the ^{58}Fe(p, n)^{58}Co spectra. As in the previous zero-degree spectrum, the excitation of the IAS at $E_x = 5.80$ MeV is the dominant feature. Differential cross sections for neutron groups below this state are presented in fig. 6. For excitation energies above the IAS, differential cross sections for 1 MeV bins were used to estimate the $\Delta L =$ contributions in the zero-degree spectrum. A summary of the observed GT strength is presented in table 5.

4. Discussion

4.1. DWIA CALCULATIONS

Microscopic calculations for the differential cross sections were done using the code DWBA-70 [21]). Values for optical model potential (OMP) parameters were obtained from ref. [22]). The effective interaction used was that parameterized from the free nucleon-nucleon interaction by Love and Franey [23]) at $E_p = 140$ MeV. More recent values for this interaction reported by Franey and Love [24]) give essentially the same results. The $\Delta J^\pi = 1^+$ transitions studied in this experiment are mainly (1f-particle) (1f-hole). Harmonic-oscillator shell-model wave functions were assumed for these transitions. For the oscillator size parameter a, we used the general

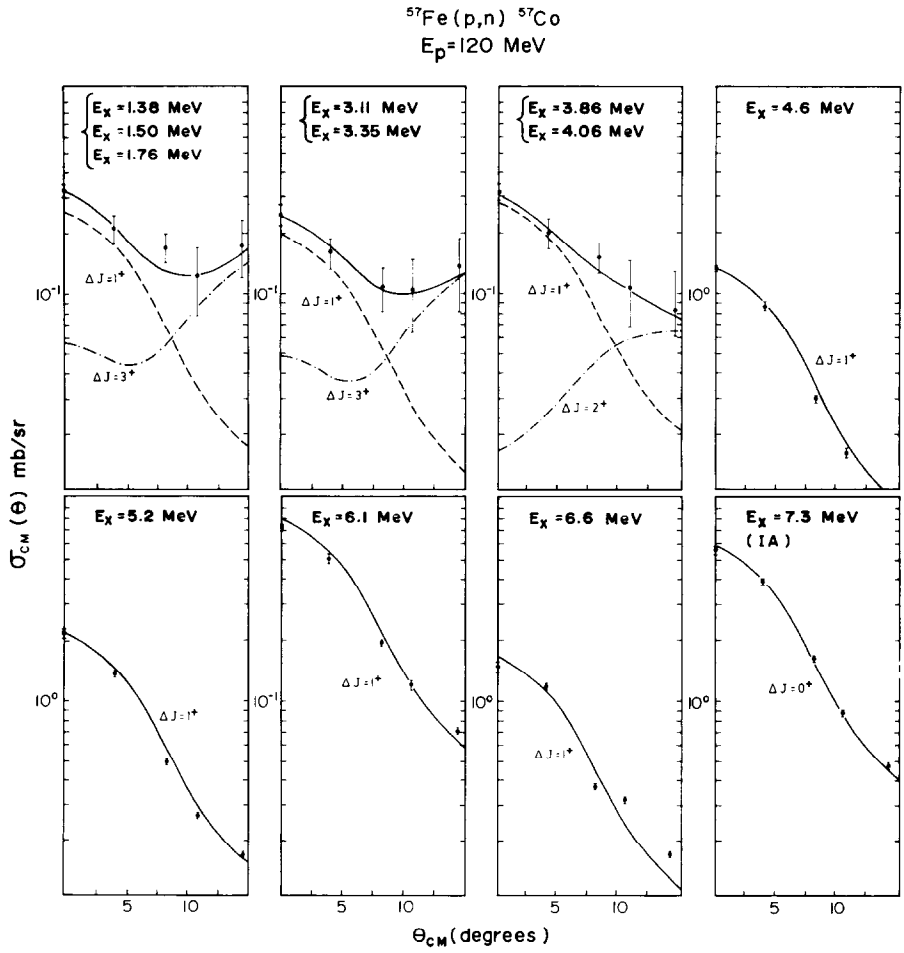

Fig. 5. Angular distributions for neutron groups observed in the ^{57}Fe(p, n)^{57}Co reaction at $E_p = 120$ MeV. The lines represent DWIA calculations for the indicated ΔJ transfers.

formula of Blomqvist and Molinari [25]):

$$a^{-2} = (0.9A^{1/3} + 0.7)\ \text{fm}^2.$$

Many of the 1^+ low-lying states in these nuclei are fairly well described with the simple (1f) shell-model space. At higher excitation, other configurations are important. For excited states with a large GT strength, the calculated shell-model wave functions (see sect. 4.3) were used to calculate the shape of the angular distributions at several excitation energies. Negative-parity transitions were assumed to be ($1g_{9/2}$ particle) ($1f_{7/2}$ hole) configuration. The shapes indicated in figs. 3–6 represent some of these calculations.

TABLE 4

^{57}Fe(p, n)^{57}Co reaction ($E_p = 120$ MeV)
$L = 0$ transitions
Zero-degree cross sections and transition strengths

Neutron group E_x(MeV) [a])	$\sigma_{c.m.}(0°)$ [b]) (mb/sr)	B(GT)	B(F)
1.38, 1.50, 1.76	0.32	0.059	
3.11, 3.35	0.25	0.047	
3.86, 4.06	0.32	0.059	
4.6	1.3	0.25	
5.2	2.2	0.42	
6.1	0.74	0.14	
6.6	1.5	0.29	
7.3 [d])	5.6		5.0
7.0, 20.0		8.9 [c])	
		$\sum B(\mathrm{GT}) = 10.2 \pm 2.6$	

[a]) Estimated location of neutron group centroid; uncertainty ±0.1 MeV.
[b]) Estimated cross-section of corresponding neutron group; uncertainty ±15%.
[c]) Value calculated using 1 MeV interval histogram (see fig. 7).
[d]) Isobaric analog transition.

4.2. GT STRENGTH FUNCTION AND SUM RULE

Zero-degree (p, n) cross sections are usually used to obtain estimates of transition strengths for $\Delta L = 0$ transitions [1]). However, there can be zero-degree contributions arising from other multipolarities. To empirically estimate the "background" contributions due to processes other than Fermi or GT transitions, we have used the procedures indicated in ref. [12]) which require the use of empirical angular distributions and DWBA-70 calculations for shapes of several multi-polarities. After removing the peak corresponding to the Fermi transition (IAS) the results that represent just GT strength are shown in figs. 7–8.

As reported in refs. [1,26,27]) the low-momentum transfer (p, n) cross section for GT or F transitions can be represented as a product of three factors:

$$\sigma_\alpha(q, \omega) = \hat{\sigma}_\alpha(A) F(q, \omega) B(\alpha) , \qquad (1)$$

where $\alpha =$ GT or F. The factor $\hat{\sigma}_\alpha(A)$ is a nuclide-dependent proportionality factor cross section per unit strength ("unit cross sections"), $F(q, \omega)$ describes the dependence on the momentum transfer q and energy loss ω and is identical to unity in

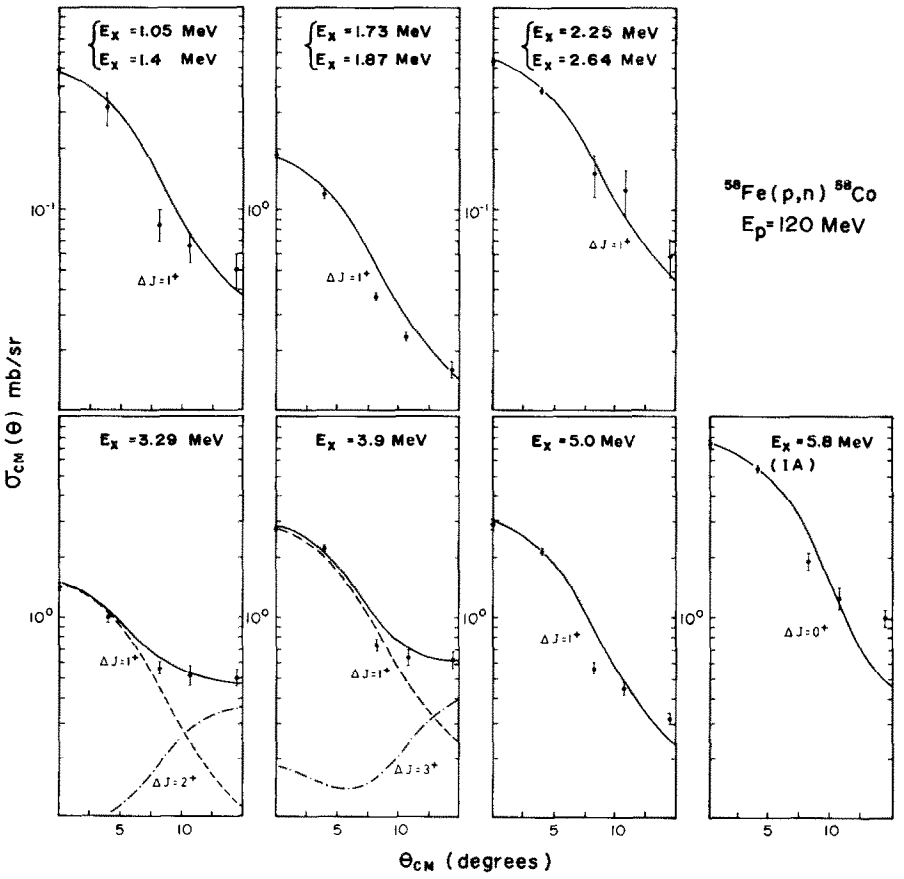

Fig. 6. Angular distributions for neturon groups observed in the ^{58}Fe(p, n)^{58}Co reaction at $E_p = 120$ MeV. The lines represent DWIA calculations for the indicated ΔJ transfers.

the limit $(q, \omega) \to 0$, and $B(\alpha)$ is the reduced transition strength:

$$B(\mathrm{GT}) = \frac{1}{(2J_i + 1)} \left| \langle \mathrm{f} \| \sum_k \sigma_k \tau_k^- \| \mathrm{i} \rangle \right|^2$$

or

$$B(\mathrm{F}) = \frac{1}{(2J_i + 1)} \left| \langle \mathrm{f} \| \sum_k \tau_k^- \| \mathrm{i} \rangle \right|^2$$

for the Gamow-Teller $\alpha = \mathrm{GT}$, or Fermi $\alpha = \mathrm{F}$ transition as defined, for instance, in Bohr and Mottelson [28]) for β-decay transitions. The summation is over all nucleons in the nuclide. In the case of β-decay, these reduced transition probabilities may

TABLE 5

^{58}Fe(p, n)^{58}Co reaction ($E_p = 120$ MeV)
$L = 0$ transitions
Zero-degree cross sections and transition strengths

Neutron group E_x (MeV) [a]	$\sigma_{c.m.}(0°)$ [b] (mb/sr)	B(GT)	B(F)
1.05, 1.38, 1.44	0.49	0.094	
1.73, 1.87	1.8	0.35	
2.25, 2.64	0.53	0.1	
3.29	1.4	0.27	
3.9	2.7	0.54	
5.0	2.9	0.60	
5.8 [d]	7.3		6.0
5.5, 20.0		13.7 [c]	
		$\sum B(\mathrm{GT}) = 15.9 \pm 3.8$	

[a]) Estimated location of neutron group centroid; uncertainty ±0.1 MeV.
[b]) Estimated cross section of corresponding neutron group; uncertainty ±15%.
[c]) Value calculated using 1 MeV interval histogram (see fig. 7).
[d]) Isobaric analog transition.

be obtained directly from ft-values according to the expression [28]):

$$B(\mathrm{F}) + \left(\frac{g_A}{g_V}\right)^2 B(\mathrm{GT}) = \frac{6143.4 \pm 3.8}{ft}.$$

The value 6163.4±3.8 is the vector coupling constant determined by Hardy and Towner [29]). The quantity (g_A/g_V) is the ratio of the axial to the vector coupling constant and is taken as [30]) 1.250±0.009.

The proportionality factor $\hat{\sigma}_\alpha(A)$ used to convert measured cross sections to transition strengths may be obtained empirically in two ways. If a transition is observed both in β-decay and in intermediate energy (p, n) reaction, the B(GT) obtained from the ft-value and the measured zero-degree cross section may be used in eq. (1) to obtain a "unit cross section value" $\hat{\sigma}_{GT}(A)$ for the nuclide under study. The factor $F(q, \omega)$ is generally close to unity and can be calculated with small uncertainty [1]). Another method is to use the empirically determined ratio $\hat{\sigma}_{GT}/\hat{\sigma}_F$ [refs. [1,31])]. This ratio (at incident energies $50 \leq E_p$ (MeV) ≤ 200) can approximately be written:

$$\frac{\hat{\sigma}_{GT}}{\hat{\sigma}_F} \simeq \frac{\sigma_{GT}(0°)}{\sigma_F(0°)} \frac{B(\mathrm{F})}{B(\mathrm{GT})} = R^2,$$

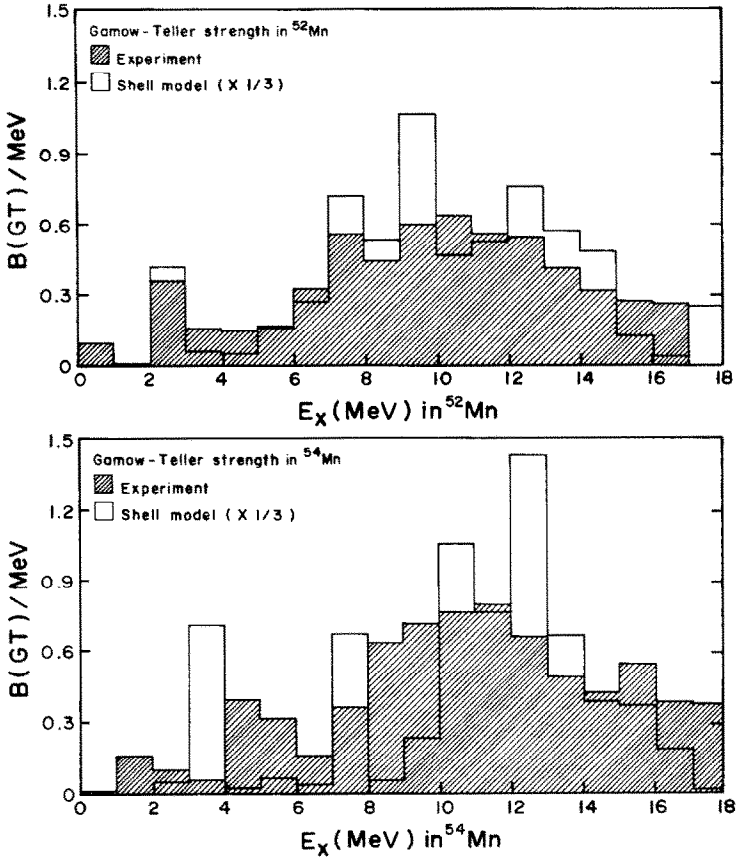

Fig. 7. Gamow-Teller strength for the (top) ^{52}Cr(p, n)^{52}Mn and (bottom) ^{54}Cr(p, n)^{54}Mn reactions. The strength in energy bins of 1 MeV is presented versus excitation energy. The experimental B(GT) (shaded area) is compared with shell-model calculations that have been multiplied by $\frac{1}{3}$.

where $\sigma_{GT}(0°)$ and $\sigma_F(0°)$ correspond to the measured zero-degree cross sections for states containing GT and F strength, respectively. For incident energies $50 \leq E_p \leq 200$, it has been shown [1]) that this ratio is described by the nuclide-independent value:

$$R = E_p(\text{MeV})/(55 \pm 1\ \text{MeV}) .$$

If the IAS transition is resolved, the measured cross section $\sigma_F(0°)$ and the value $B(F) = (N - Z)$ may thus be used to obtain the required cross section per unit GT strength, $\hat{\sigma}_{GT}$. Calculable correction factors $F(q, \omega)$ should contribute only small uncertainties in this procedure.

Both methods were used and gave consistent results within 10% deviation. The GT excitation functions in B(GT) units such that for the free neutron $B(GT) = 3$, are shown in figs. 7-8.

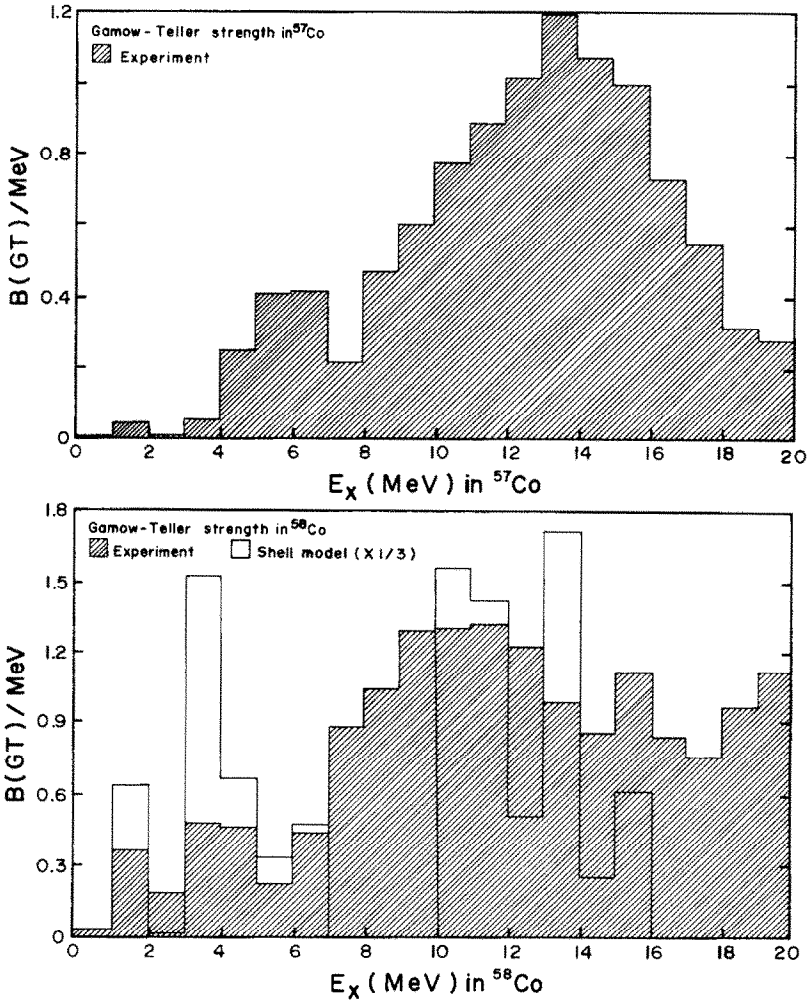

Fig. 8. Gamow–Teller strength for the (top) ^{57}Fe(p, n)^{57}Co and (bottom) ^{58}Fe(p, n)^{58}Co reactions. The strength in energy bins of 1 MeV is presented versus excitation energy. The shell-model strength for the ^{58}Fe(p, n)^{58}Co reaction multiplied by $\frac{1}{3}$ is compared (bottom) with the experimental B(GT) (shaded area).

A simple model independent sum rule [2]) may be used to determine the expected GT strength:

$$S_{\beta^-} - S_{\beta^+} = 3(N - Z) .$$

In heavy nuclei S_{β^+} is expected to be negligible due to Pauli blocking effects. For the 1f shell nuclei studied here $f_{5/2}$ vacancies exist for both neutrons and protons so both S_{β^-} and S_{β^+} will be non-zero. The total β^- strength is then $S_{\beta^-} = [3(N - Z) + S_{\beta^+}]$. There are no experimentally determined GT$^+$ strengths for nuclei

in this study, except for $A = 54$ [ref. [6])]. We use shell-model calculations, which are consistent with the sum rule, to estimate the S_{β^-} and S_{β^+} values. The excitation function for the $B(GT^-)$ shell-model calculations are compared to the data in figs. 7–8. Both the GT^- empirical strength and theoretical calculations strength have been summed up in 1 MeV energy bins to make the comparison.

4.3. SHELL-MODEL CALCULATIONS

In this section we present the corresponding shell-model calculations for charge-exchange reactions and shell-model calculations for M1 excitations for the case of ^{52}Cr.

Low-lying levels of nuclei with $1f_{7/2}$ valence nucleons such as ^{52}Cr and ^{54}Fe are fairly well described with the simple $1f_{7/2}$ model space (model space A) [32]). However, this basis is not adequate for the calculation of GT strength because of the importance of the $1f_{7/2}$ to $1f_{5/2}$ transitions. Also, in the case of ^{54}Cr and ^{57,58}Fe, transitions within the 2p shell are required. Since a full basis (fp) shell-model calculation is prohibitive, we have adopted a model-space truncation which allows at most one particle to be excited. This model space is called B. For all the calculations, we use the van Hees and Glaudemans interaction [33]).

For the g.s. of ^{58}Fe we have assumed a simple 4-particle 2-hole (4p2h) configuration to calculate the GT^- strength function. Because of the large dimension involved, we have not done the shell-model calculations for the ^{57}Fe(p, n)^{57}Co reaction.

The calculations were carried out with the shell-model code OXBASH [34]). In the next subsections we present results for the individual cases.

4.3.1. *Results for ^{52}Cr.* Within the assumption that GT transitions occur in the A → B model spaces defined above, excited states up to 18 MeV excitation in ^{52}Mn carry all the calculated GT^- strength. The sum strength in 1 MeV energy bins is compared with the data also summed in 1 MeV bins in fig. 7. The calculated curve has been scaled by a factor of $\frac{1}{3}$ to make the shape comparison more apparent. In table 6 we list the sum of the experimental and calculated results for the $B(GT^-)$

TABLE 6

Summary of GT strengths

Target	S_{β^-}			S_{β^+}	
	observ.	calc.	Q_{GT} [a]) (Model space A → B)	observ.	calc.
^{52}Cr	5.9 ± 1.5	18.9	0.31		6.9
^{54}Cr	7.7 ± 1.9	20.5	0.38		2.5
^{57}Fe	10.2 ± 2.6				
^{58}Fe	15.9 ± 3.8	31.6 [b])	0.50		13.6 [b])

[a]) Defined as the ratio between the observed and calculated sum GT-strength.

[b]) Assuming a simple shell-model space ("zero-order" model).

strength. A shell-model calculation also assuming A→B model spaces, have been reported for the ^{52}Cr(p, n)^{52}Mn reaction in ref. [9]). The only difference is in the adopted effective interaction. The excitation function for the GT$^-$ strength is very similar to the one reported here and the reported sum GT$^-$ strength is shown in table 6.

We also have calculated the M1 excitation in ^{52}Cr and the results are presented in sect. 4.4.

4.3.2. Results for A = 54.

(a) ^{54}Cr(p, n)^{54}Mn. Shell-model calculations for the GT$^-$ strength were done assuming that the ^{54}Cr g.s. wave function has a $[(\pi f_{7/2})^4 (\nu f_{7/2})^8 (\nu x^2)]_{0^+}$ configuration with $x = p_{3/2}$, $f_{5/2}$ and $p_{1/2}$ with neutron occupation probabilities of 81.5%, 14.3% and 4.2%, respectively. The 1^+ states in ^{54}Mn were calculated to all possible configurations that could be reached by moving one nucleon from the assumed ^{54}Cr g.s. configuration. This involved a dimension of 809. The sum strength in 1 MeV energy bins is compared with the data also summed in 1 MeV bin in the lower half of fig. 7.

(b) ^{54}Fe(n, p)^{54}Mn. The $B(GT)^-$) and $B(GT^+)$ strength distributions leading to the same final nucleus are important in double beta-decay calculations (see sect. 4.5.). In this case, some of the final states in ^{54}Mn, in particular low-lying states, should be populated both in the ^{54}Cr(p, n)^{54}Mn and in the ^{54}Fe(n, p)^{54}Mn reactions. Of course, the GT strengths in both directions are not the same because of the different g.s. configurations of ^{54}Cr and ^{54}Fe. Calculations for the (GT$^-$) strength to final states in ^{54}Mn are described in the above paragraph. In this section we present results for the calculated (GT$^+$) strength to final states in ^{54}Mn.

Calculations for the $B(GT^+)$ strength distribution also have been done by Bloom and Fuller [35]) and by Muto *et al.* [36]).

We have assumed in our calculations that the ^{54}Fe g.s. wave function may be described by a pure 0p2h model, i.e., $[(\pi f_{7/2})^{-2}(\nu f_{7/2})^8]_{0^+}$ which is essentially a "zero-order" model. The application of the GT$^+$ operator to this state produces six $J^\pi = 1^+$ states which, using the van Hees interaction, are all located below 6 MeV of excitation energy. A similar distribution is predicted by Bloom and Fuller and both calculations give a total strength $S_{\beta^+} = 10.29$.

Bloom and Fuller [35]) and Muto [36]) have assumed in addition, a 1p3h configuration for the ground state wave function of ^{54}Fe leading to 1^+ states in ^{54}Mn with configurations up to 2p4h. The GT$^+$ strength is still mainly concentrated in the first few MeV of excitation and the sum (n, p) strength is reduced by about 10%, $S_{\beta^+} = 9.12$ [ref. [35])]. We do not pursue these calculations because the additional ph configurations would require an even larger dimension than the one used in refs. [35,36]) for the calculation of the ^{54}Cr(p, n)^{54}Mn GT$^-$ strength.

4.3.3. Results for A = 58.

(a) ^{58}Fe(p, n)^{58}Co. Shell-model calculations for the GT$^-$ strength were done assuming that the ^{58}Fe g.s. wave function has a simple 4-particle 2-hole configuration.

The results indicate that excited states up to 16 MeV in ^{58}Co carry all the GT$^-$ strength. The sum strength in 1 MeV energy bins is compared with the data also summed in 1 MeV bins in the lower half of fig. 8. The large empirical GT$^-$ strength observed above 16 MeV excitation energy in ^{58}Co indicates the simplicity of the adopted model space. However, the large dimensions involved make prohibitive a calculation in a larger shell-model space. The calculated S_{β^-} and S_{β^+} strengths are presented in table 6.

(b) ^{58}Ni(n, p)^{58}Co. As it was the case for $A = 54$, final states in ^{58}Co may be reached via the ^{58}Fe(p, n) and ^{58}Ni(n, p) reactions. Even though the experimental data are not yet available, we have performed a shell-model calculation for the ^{58}Ni(n, p)^{58}Co reaction, again in a simple model. The results indicate that the GT$^+$ strength is concentrated below 4 MeV of excitation and that the calculated sum strength is $S_{\beta^+} = 13.2$

4.4. COMPARISON WITH OTHER PROBES

Extensive data are available for the M1 excitation in ^{52}Cr via (e, e′) and (p, p′) reactions. In this section, we compare such data with the present results and with shell-model calculations. There are no similar data for the other nuclei studied in this paper.

The GT excitation function derived from the ^{52}Cr(p, n) data is presented in fig. 9 and is compared with the M1 strength distribution in ^{52}Cr as measured by the (e, e′) reaction [9]) as well as by the ^{52}Cr(p, p′) cross section measured at $\theta_L = 4°$ and $E_p = 201$ MeV [ref. [8])]. The portion of the (p, p′) spectrum between 9–12 MeV in ^{52}Cr is reported [8]) to have $T = 2$. Two states at 12.56 and 12.90 MeV excited in the (p, p′) reaction have been classified [8]) as having $T = 3$.

In principle isobaric analogs of the M1 states, excited via the spin-isospin interaction with intermediate energy protons should be excited in the (p, n) reaction. However, because of the small values of the isospin Clebsch-Gordon coefficients, the (p, n) cross sections for exciting $T = 3$ states relative to $T = 2$ states are strongly reduced. The analogs of states in ^{52}Mn should be located at excitation energies that are 2.925 MeV larger than those of their parent states in ^{52}Cr. Although the energy resolution is better for the (p, p′) work than in the present (p, n) study, it can be seen in fig. 9 that the structure observed in the (p, n) spectrum between 11.9–15.0 MeV is similar to that of the (p, p′) spectrum in the corresponding energy region 9–12.1 MeV. From an analysis of the (p, n) spectrum using gaussian peak shapes, we find good correspondence with the (p, p′) data. In fact the relative cross sections found for the (p, n) neutron groups were very similar to those for the (p, p′) data. We did not observe the analogs for the two $T = 3$ peaks observed in the (p, p′) work. This is in accordance with the expectations based upon the relative magnitudes of the Clebsch-Gordon coefficients as noted above. The good agreement between the excitation energies and relative cross sections of the peaks observed in the (p, p′)

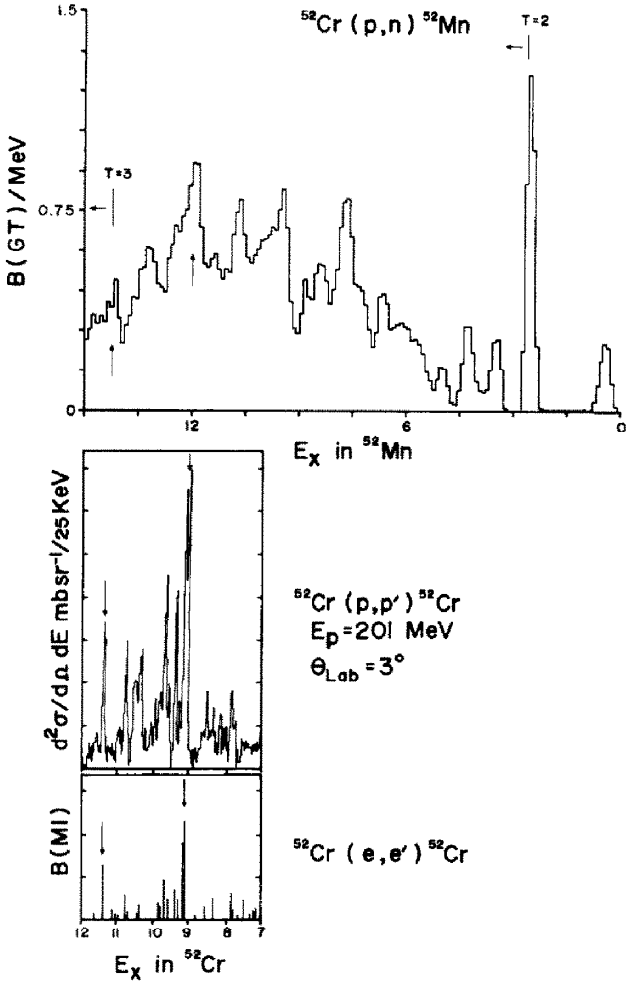

Fig. 9. Comparison of the excitation of 1^+ states in ^{52}Cr via the (p, p') [ref. [8])] and (e, e') [ref. [9])] reactions with 1^+ states in ^{52}Mn excited in the (p, n) reaction.

and (p, n) reactions seems to suggest that the (p, n) cross section in the 12–15 MeV energy region are dominated by $T = 2$ states. We have calculated $B(\mathrm{M1})\uparrow$ from the $B(\mathrm{GT})$ values assuming $T = 2$ states. These are tabulated in table 7 and compared with $B(\mathrm{M1})\uparrow$ deduced from the (e, e') data. In the energy interval considered here, we find $\sum_{\mathrm{pn}} B(\mathrm{M1})\uparrow = 4.7\ \mu_n^2$ and $\sum_{\mathrm{e,e'}} B(\mathrm{M1})\uparrow = 4.75\ \mu_n^2$ if we only include definite M1 states. Assuming that the M1 states observed in the (e, e') reaction are excited only via the spin-isospin interaction, this would suggest that the states excited in the (p, n) reaction are mainly $T = 2$ states, whereas the theoretical calculations

TABLE 7

Comparison of $B(M1\uparrow)$ in ^{52}Cr from (e, e') measurements with $B(M1)\uparrow$ deduced from the $^{52}Cr(p, n)^{52}Mn$ reaction

(e, e')		(p, n) [c]		
$E_x(^{52}Cr)$ (MeV)	$B(M1)$ (μ_n^2)	$E_x(^{52}Cr)$ (MeV)	$B(GT)$	$B(M1)$ [c] (μ_n^2)
9.14	1.12			
		12.0	0.216	1.14
9.21	0.88			
9.32	0.23			
		12.3	0.118	0.62
9.42	0.24			
9.61	0.23	12.5	0.045	0.24
9.72	0.43	12.6	0.10	0.53
9.83	0.15	12.8	0.025	0.13
9.88	0.18			
		12.9	0.05	0.26
10.0	0.05			
10.27(?) [b]	0.13			
10.34(?)	0.19			
10.38(?)	0.20	13.2	0.073	0.38
10.43	0.17			
10.46	0.07			
10.51(?)	0.18	13.4	0.073	0.38
10.61(?)	0.04			
10.71	0.08			
10.76	0.044			
		13.6	0.064	0.34
10.79	0.26			
10.82(?)	0.036			
10.92(?)	0.068			
		13.9	0.057	0.30
11.07(?)	0.065			
11.14(?)	0.12			
11.40	0.62	14.3	0.068	0.38
Sum:	5.78 (all transitions)	Sum:	0.89	4.7
	4.75(only definite M1 states)			

[a] Ref. [8]).
[b] A question mark indicates other than M1 assignment possible.
[c] Assuming $T = 2$ states.

indicate about equal $T = 1$ and $T = 2$ GT strength in this energy interval. We have arrived at a similar conclusion by using DWIA calculations to scale the 4° (p, p') cross section [8]) at 201 MeV to equivalent values at 0° cross sections at 120 MeV. If the states observed in the (p, n) reaction are isobaric analogs of the $T = 2$ states excited in the (p, p') reaction, then $\sigma_{pn}(0°)$ should equal $\sigma_{pp'}(0°)$ for the same incident energy. From the (p, p') data [8]) we deduce $\sum_{T=2} \sigma_{pp'}(0°)_{120MeV} \cong 4.42$ mb/sr, which

is in good agreement with our measured value $\Sigma\sigma_{pn}(0°) = 3.91$ mb/the latter is a sum over the levels tabulated in table 7.

4.5. (p, n) AND (n, p) REACTIONS

4.5.1. The (p, n) and (n, p) reactions on ^{54}Fe. As indicated in sect. 4.1., the zero-degree (p, n) spectra at intermediate energies provide unique information on the energy distribution of the GT^- strength, while (n, p) data on the same target should provide information on the GT^+ strength. Such data exist for ^{54}Fe; the ^{54}Fe(p, n)^{54}Co data have been reported in ref. [12]) while the ^{54}Fe (n, p)^{54}Mn reaction have been studied by Vetterli *et al.* [6]) at $E_n = 298$ MeV.

A summary of the experimental and calculated results are shown in table 8.

For ^{54}Fe S_{β^+} is large and model sensitive. Thus, it follows from the sum rule that the calculated value of S_{β^-} is also model sensitivite and a comparison with the empirical $\sum B(GT^-)$ to obtain a quenching factor cannot be stated with certainty. The calculated value in a "zero-order" model is 16.29. Using 0p2h and 1p3h configurations for the ^{54}Fe g.s. wave function, a value 15.21 is obtained [35]). The empirical value $\sum B(GT^-) = 7.8 \pm 1.9$ is reported in ref. [12]).

TABLE 8

Sum rule GT strength for ^{54}Fe

^{54}Fe(p, n) S_{β^-}		^{54}Fe(n, p) S_{β^+}	
observ.	calc.	observ.	calc.
7.8 ± 1.9	16.29	3.8 [a])	10.29
		5.2 [b])	
		3.3 [c])	
	15.21 [d])		9.1 [d])

[a]) Value from ref. [6]).
[b]) From ^{54}Fe(e, e') data. See text.
[c]) From ^{54}Fe(p, p') data. See text.
[d]) From ref. [35]) using 0p2h and 1p3h configurations for the ^{54}Fe g.s. wave function. A 0p2h ("zero-order" model) gives the values indicated in the first row.

Our calculated value in the "zero-order" model for S_{β^+} is 10.29. Vetterli *et al.* [6]) estimate the $\sum B(GT^+)$ value from the measured 12.9 ± 1.2 mb/sr $\Delta L = 0$ cross section below 10 MeV excitation energy in ^{54}Mn, obtained in the zero-degree ^{54}Fe(n, p)^{54}Mn reaction at 298 MeV. They estimate the GT^+ strength by evaluating the "unit cross section" theoretically. A value $\sum B(GT^+) = 3.8 \pm 0.4$ is obtained and including a systematic error of 0.6 arising from the estimation of the unit cross section a value

$\sum B(GT^+) = 3.8 \pm 0.4 \pm 0.6$ is quoted [6]). The empirical values from the sum GT^- and GT^+ strengths are a fraction of the calculated values. Thus, even if we say that the shell-model space used in the calculations is not adequate, we still must conclude that we have not found all the GT strength. It is most plausible to say, however, that both the GT^- and GT^+ strengths are quenched. Unfortunately, the above results do not test the sum rule. The quenching we calculate for the GT^- and GT^+ strengths are rather different whether is comes from redistribution of strength due to 2p2h coupling in the excitation energy below 100 MeV or whether the delta polarizes the nucleus so that the $\sigma\tau$ operator is renormalized.

Another estimate of S_{β^+} may be obtained from the ^{54}Fe(e, e') result of Sober *et al.* [9]). Using the value $\sum B(M1)\uparrow = 5.5\ \mu_n^2$ reported for levels with a "*unique*" M1 multipole assignment and the calculated shell-model value for $T = 2$ states of $\sum B(M1)\uparrow = 10.9\ \mu_n^2$, a quenching of $(5.5/10.9) = 0.51$ is obtained. This factor can be different from the GT quenching factor because orbital currents contribute to M1 strength and not to GT strength.

We can get another estimate of S_{β^+} from the ^{54}Fe(p, p') data [8]). Assuming that the states above 9.94 MeV reported in ref. [8]) are $T = 2$ states the sum $\sum \sigma(4°)$ for all these states is 2.89 mb/sr [table 3, ref. [7])]. The calculated $\sum$ (p, p') cross section for these states gives a value $\sum \sigma_{cal}(4°) = 9.05$ mb/sr which would imply a quenching of $Q_{pp'} = (2.89/9.05) = 0.32$.

4.5.2. The (p, n) and (n, p) reactions to final states in ^{54}Mn. We present in table 9 the observed and calculated GT strengths for states in ^{54}Mn populated via the

TABLE 9

Low-lying GT states in ^{54}Mn reached via (p, n) and (n, p) reactions

^{54}Mn E_x(MeV)		^{54}Cr(p, n) B(GT)		^{54}Fe(n, p) (GT)	
observ.	calc.	observ.	calc. [a])	observ.	calc. [a])
1.40	1.40	0.12	0.003		0.64
1.90	2.11	0.084	0.002		0.39
2.60	2.36	0.064	0.012		1.46
2.90	3.07		0.008		3.07
4.10	3.82		0.011		1.85
4.30		0.45			
4.70					
5.4		0.45			
5.7					
	6.04		0.002		2.88
	Sum:	1.17	0.038	3.8 [b])	10.29

[a]) Calculated using the "zero-order" model with interaction of ref. [32]).

[b]) Value for the sum strength reported in ref. [5]) up to 8.0 MeV excitation energy.

^{54}Cr(p, n) and ^{54}Fe(n, p) reactions. The GT matrix elements that we can empirically obtain from these reactions are important in the calculations involving double beta-decay. For ^{54}Fe, double electron capture is the only open second-order weak decay mode. These processes are important during the late stages of stellar evolution as pointed out by Bethe *et al.* [38]). Values obtained from the present study for the B(GT) excitation function and the zero-degree ^{54}Fe(n, p) spectrum obtained with 298 MeV neutrons [6]) are presented in fig. 10. It seems that only states up to about 5 MeV excitation energy in ^{54}Mn have an overlap in both channels. The calculated B(GT) values using the "zero-order" model are presented in table 9. The comparison between the empirical and calculated values for the ^{54}Cr(p, n) B(GT) indicates that such a model is not adequate for this double-beta decay calculation. Even including an additional 1p1h configuration [35]) in the g.s. wave function for ^{54}Fe will not be sufficient because in the simple shell-model picture, the g.s. wave function for ^{54}Cr requires 2p4h configurations. The GT operator will also produce 3p5h states in ^{54}Mn which must be included. Thus this comparison indicates clearly the important of empirical GT matrix elements for these type of calculations.

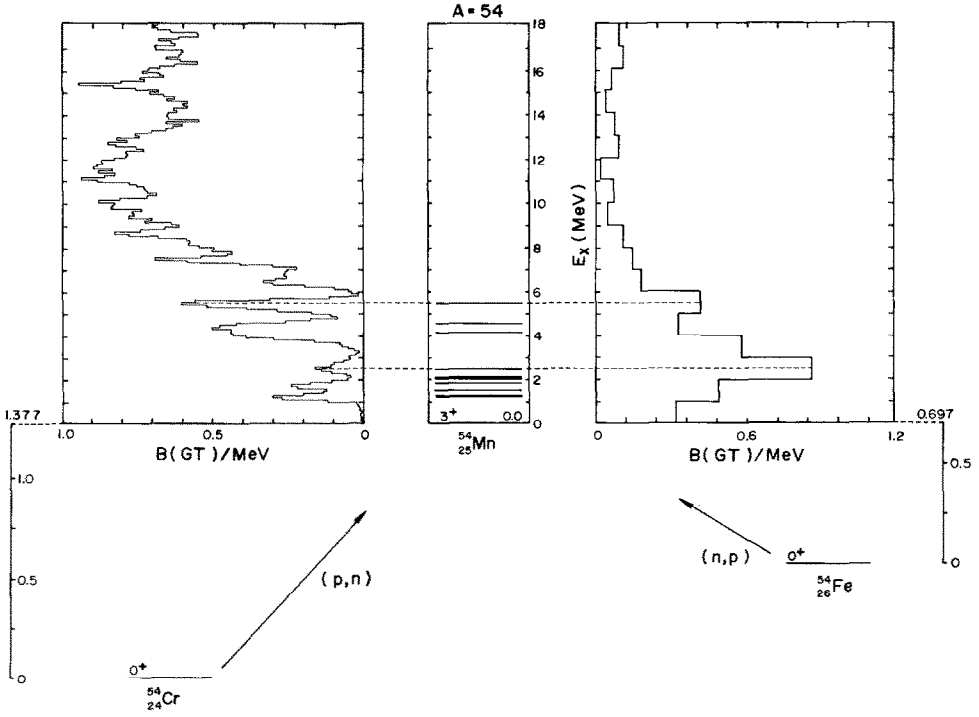

Fig. 10. Excitation of 1^+ states in ^{54}Mn excited in the ^{54}Fe(n, p) reaction [(ref. [6])] and in the ^{54}Cr(p, n) reaction (this work). The GT strength per MeV is presented versus excitation energy in ^{54}Mn. The reported 1^+ states in ^{54}Mn [ref. [20])] are presented as solid lines. The dashed lines indicate group of states that seem to be populated in both reactions.

5. Summary and conclusions

The excitation function for the (p, n) GT strength in the nuclei ^{52,54}Cr and ^{57,58}Fe have been studied up to approximately 20 MeV excitation energy and compared with shell-model calculations. A summary of these results are compared with similar data for other $1f_{7/2}$ nuclei in table 10.

A comparison among the $N = 28$ isotones indicates a sharp decrease in the empirical GT strength (observed up to 20 MeV excitation) with the filling of the $1f_{7/2}$ proton subshell. Assuming a simple shell-model space, the calculated (p, n) sum strength does not decrease as much as this is reflected in the large variations observed in the values of Q_{GT} (table 10). For the Fe isotopes, the empirical GT$^-$ strength, as expected, increases with mass number. The theoretical GT strength increases in about the same proportion, which is reflected in the same value $Q_{GT^-} \approx 0.5$ for all the isotopes.

The large variation of Q_{GT} values (table 10) deserves further explanation. Of course, additional GT strength may possibly reside in many small transitions above 20 MeV excitation energy, but the theoretical results using the truncated shell-model spaced indicated in sect. 4.3 indicate almost no GT strength above 20 MeV. It is indicated in ref. [5]) that correlations in the g.s. wave function in a $0\hbar\omega$ shell-model space will reduce the calculated (p, n) GT strength as compared with the results obtained using the "zero-order" approximation. If the shell-model space is increased

TABLE 10

Summary of sum (p, n) GT strength for some $1f_{7/2}$ nuclei

	Empircal		Calculated	$Q_{GT} = \sum B(GT)/S_{\beta^-}$
	$\sum B(GT)^-$	ref.	S_{β^-} [a])	
N = 28 isotones				
^{48}Ca(p, n)^{48}Sc	17^{+2}_{-3}	5, 11	24	$0.71^{+0.08}_{-0.13}$
$^{51}_{23}$V(p, n)^{51}Cr	12.6 ± 2.5	5	20.14	0.63 ± 0.13
$^{52}_{24}$Cr(p, n)^{52}Mn	5.9 ± 1.5	this	18.9	0.31 ± 0.08
$^{54}_{26}$Fe(p, n)^{54}Co	7.8 + 1.9	12	16.3	0.48 ± 0.12
Other $1f_{7/2}$ nuclei				
$^{40}_{20}$Ca(p, n)^{40}Sc	0,1	39	0.0	
$^{42}_{20}$Ca(p, n)^{42}Sc	$4.2^{+0.2}_{-0.5}$	40	6.0	$0.7^{+0.03}_{-0.08}$
$^{54}_{24}$Cr(p, n)^{54}Mn	7.7 ± 1.9	this	20.5	0.38 ± 0.09
$^{56}_{26}$Fe(p, n)^{56}Co	9.9 ± 2.4	12	22.1	0.45 ± 0.11
$^{57}_{26}$Fe(p, n)^{57}Co	10.2 ± 2.6	this		
$^{58}_{26}$Fe(p, n)^{58}Co	15.9 ± 3.8	this	31.6	0.5 ± 0.12
$^{58}_{28}$Ni(p, n)^{58}Cu	7.4 ± 1.8	12	19.2	0.39 ± 0.09
$^{60}_{28}$Ni(p, n)^{60}Cu	7.2 ± 1.8	12	24.6	0.29 ± 0.07

[a]) Shell model calculated (p, n) sum strength assuming the simplest configuration ("zero order" model).

to several $\hbar\omega$, the energy distribution of the GT strength will also be affected giving a different sum up to 20 MeV excitation energy.

For $A = 54$, GT quenching defined as the empirical $\sum B(\mathrm{GT})$ strength value divided by the calculated value can be determined from three different experiments:

$$^{54}\mathrm{Fe(p, n)}^{54}\mathrm{Co}\,,\ Q_{\mathrm{GT}} = 0.48 \qquad \text{(see table 10)}\,,$$

$$^{54}\mathrm{Fe(n, p)}^{54}\mathrm{Mn}\,,\ Q_{\mathrm{GT}} = 0.37 \qquad \text{(see table 8)}\,,$$

$$^{54}\mathrm{Cr(p, n)}^{54}\mathrm{Mn}\,,\quad Q_{\mathrm{GT}} = 0.38 \qquad \text{(see table 10)}\,.$$

Finally, the importance of empirical GT matrix elements for the evaluation of double beta decay is presented, citing as an example the case for ^{54}Fe.

This work was supported in part by the National Science Foundation, the US Department of Energy and the Danish Science Research Council. The careful target preparations by W. Lozowski and maintenance of the neutron detectors by K. Komisarcik both at IUCF are deeply appreciated.

References

1) T.N. Taddeucci, C.A. Goulding, T.A. Carey, R.C. Byrd, C.D. Goodman, C. Gaarde, J. Larsen, D. Horen, J. Rapaport and E. Sugarbaker, Nucl. Phys. **A469** (1987) 125;
C.D. Goodman *et al.*, Phys. Rev. Lett **44** (1980) 1755
2) C. Gaarde, J.S. Larsen, M.N. Harakeh, S.Y. van der Werf, M. Igarashi and A. Muller-Arnke, Nucl. Phys. **A334** (1980) 248;
See also M.H. MacFarlane, Phys. Lett. **182B** (1986) 265
3) C. Gaarde, J.S. Larsen and J. Rapaport, Spin excitations in nuclei, ed. F. Petrovich, G.E. Brown, G.T. Garvey, C.D. Goodman, R.A. Lindgren and W.G. Love (Plenum, New York, 1984), p. 65;
C.D. Goodman and S.D. Bloom in *op. cit.*, p. 143
4) G.F. Bertsch and H. Esbensen, Rep. Prog. Phys. **50** (1987) 607
5) J. Rapaport, R. Alarcon, B.A. Brown, C. Gaarde, J. Larsen, C.D. Goodman, C.C. Foster, D. Horen, T. Masterson, E. Sugarbaker and T.N. Taddeucci, Nucl Phys. **A427** (1984) 332
6) M.C. Vetterli, O. Hausser, W.P. Alford, D. Frekers, R. Helmer, R. Henderson, K. Hicks, K.P. Jackson, R.G. Jeppesen, C.A. Miller, M.A. Moinester, K. Raywood and S. Yen, Phys. Lett. **59** (1987) 439
7) G. Eulenberg, D.I. Sober, W. Steffen, H.D. Graf, G. Kuchler, A. Richter, E. Spamer, B.C. Metsch and W. Knupfer, Phys. Lett. **116B** (1982) 113
8) C. Djalali, N. Marty, M. Morlet, A. Willis, J.C. Jourdain, N. Anantaraman, G.M. Crawley, A. Galonsky and P. Kitching, Nucl. Phys. **A388** (1982) 1;
C. Djalali, N. Marty, M. Morlet, A. Willis, J.C. Jourdain, N. Anantaraman, G.M. Crawley, A. Galonsky and J. Duffy, Nucl Phys. **A410** (1983) 399; **A417** (1984) 564
9) D.I. Sober, B.C. Metsch, W. Knupfer, G. Enlenberg, G. Kuchler, A. Richter, E. Spamer and W. Steffen, Phys. Rev. **C31** (1985) 2054
10) M. Fujiwara, Y. Fujita, S. Imanishi, S. Morinobu, T. Yamaraki and H. I. Kegami, Phys. Rev. **C32** (1985) 830
11) B.D. Anderson, T. Chittrakarn, A.R. Baldwin, C. Lebo, R. Madey, P.C. Tandy, J.W. Watson, B.A. Brown and C.C. Foster, Phys. Rev. **C31** (1985) 1161

12) J. Rapaport, T.N. Taddeucci, T.P. Welch, C. Gaarde, J. Larsen, D.J. Horen, E. Sugarbaker, P. Koncz, C.C. Foster, C.D. Goodman, C.A. Goulding and T. Masterson, Nucl. Phys. **A410** (1983) 371
13) I.S. Towner and F.C. Khanna, Nucl. Phys. **A399** (1983) 334
14) C.D. Goodman, C.C. Foster, M.B. Greenfield, C.A. Goulding, D.A. Lind and J. Rapaport, IEEE Trans. Nucl. Sci. **NS-26** (1979) 2248
15) C.D. Goodman, J. Rapaport, D.E. Bainum and C.E. Brient, Nucl. Instr. Meth. **151** (1978) 125; C.D. Goodman, J. Rapaport, D.E. Bainum, M.B. Greenfield and C.A. Goulding, IEEE Trans. Nucl. Sci. **NS-25** (1979) 577
16) C. Gaarde, J. Rapaport, T.N. Taddeucci, C.E. Goodman, C.D. Foster, D.E. Bainum, C.A. Goulding, M.B. Greenfield, D.J. Horen and E. Sugarbaker, Nucl. Phys. **A369** (1981) 258
17) C.A. Goulding, M.B. Greenfield, C.C. Foster, T.E. Ward, J. Rapaport, D.E. Bainum and C.D. Goodman, Nucl. Phys. **A331** (1979) 29
18) J. D'Auria, M. Dombsky, L. Moritz, T. Ruth, G. Sheffer, T.E. Ward, C.C. Foster, J.W. Watson, B.D. Anderson and J. Rapaport, Phys. Rev. **C30** (1984) 1999
19) J.R. Beene, Nucl. Data Sheets for $A = 52$, Nucl. Data Sheets **25** (1978) 235
20) W. Gongqing, Z. Jiabi and Z. Jingen, Nucl. Data Sheets for $A = 54$, Nucl. Data sheets **50** (1987) 255
21) R. Schaeffer and J. Raynal, unpublished
22) P. Schwandt, P.O. Singh, W.W. Jacobs, A.D. Bacher, P.T. Debevec, M.D. Kaitchuck and J.T. Meek, Phys. Rev. **C23** (1981) 1023; **C26** (1982) 56
23) W.G. Love and M.S. Franey, Phys. Rev. **C24** (1981) 1073
24) M.S. Franey and W.G. Love, Phys. Rev. **C31** (1985) 488
25) J. Blomqvist and A. Molinari, Nucl. Phys. **A106** (1968) 545
26) C.D. Goodman, The (p, n) reaction and the nucleon-nucleon interaction, ed. C.D. Goodman, S.M. Austin, S.D. Bloom, J. Rapaport and G.R. Satchler (Plenum, New York, 1980), p. 149
27) J. Rapaport, T.N. Taddeucci, C. Gaarde, C.A. Goulding, D. Horen, E. Sugarbaker, T.G. Masterson and D. Lind, Phys. Rev. **C24** (1981) 335
28) A. Bohr and B. Mottelson, Nuclear structure, vol 1 (Benjamin, New York, 1969), pp. 345, 349, 411
29) J.C. Hardy and I.S. Towner, Nucl Phys. **A254** (1975) 224
30) A. Kropf and H. Paul, Z. Phys. **267** (1974) 129
31) T.N. Taddeucci, J. Rapaport, D.E. Bainum, C.D. Goodman, C.C. Foster, C. Gaarde, J. Larsen, C.A. Goulding, D.J. Horen, T. Masterson and E. Sugarbaker, Phys. Rev. **C25** (1981) 1094
32) W. Kutschera, B.A. Brown and K. Ogawa, Rev. Nuovo Cim. **12** (1978) 1
33) A.G.M. van Hees and P.W.N. Glaudemans, Z. Phys. **A303** (1981) 267
34) A. Echegoyen, W.M.D. Rae and B.A. Brown, MSU-NSCL report no. 524 (1984) unpublished, The Oxford-Buenos Aires shell-model code
35) S.D. Bloom and G.M. Fuller, Nucl. Phys. **A440** (1985) 511
36) K. Muto, Nucl. Phys. **A451** (1986) 481
37) B.A. Brown and B.H. Wildenthal, Phys. Rev. **C28** (1983) 2397
38) H.A. Bethe, G.E. Brown, J. Applegate and J.M. Latimer, Nucl. Phys. **A234** (1979) 487
39) T. Chittrakarn, B.A. Anderson, A.R. Baldwin, C. Lebo, R. Madey, J.W. Watson and C.C. Foster, Phys. Rev. **C34** (1986) 80
40) C.D. Goodman, C.C. Foster, D.E. Bainum, S.D. Bloom, C. Gaarde, J. Larsen, C.A. Goulding, D.J. Horen, T. Masterson, S. Grimes, J. Rapaport, T.N. Taddeucci and E. Sugarbaker, Phys. Lett. **107B** (1981) 406;
See also J. Rapaport in AIP Conf. Proc. No. 97, ed. H. O. Meyer (AIP, New York, 1982), p. 365